Acta Crystallographica Section C
Crystal Structure Communications
ISSN 0108-2701
Editor: **Anthony Linden**

Channel-forming solvate crystals and isostructural solvent-free powder of 5-hydroxy-6-methyl-2-pyridone

Sean R. Parkin and Edward J. Behrman

Acta Cryst. (2011). C**67**, o324–o328

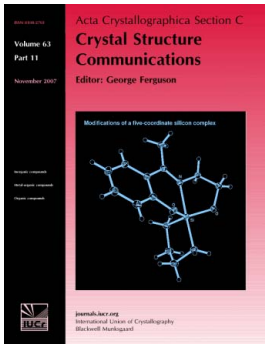

Acta Crystallographica Section C: Crystal Structure Communications specializes in the rapid dissemination of high-quality studies of crystal and molecular structures of interest in fields such as chemistry, biochemistry, mineralogy, pharmacology, physics and materials science. The numerical and text descriptions of each structure are submitted to the journal electronically as a Crystallographic Information File (CIF) and are checked and typeset automatically prior to peer review. The journal is well known for its high standards of structural reliability and presentation. *Section C* publishes approximately 1000 structures per year; readers have access to an archive that includes high-quality structural data for over 10000 compounds.

Acta Crystallographica Section C
Crystal Structure Communications
ISSN 0108-2701

Channel-forming solvate crystals and isostructural solvent-free powder of 5-hydroxy-6-methyl-2-pyridone

Sean R. Parkin[a]* and Edward J. Behrman[b]

[a]Department of Chemistry, University of Kentucky, Lexington, KY 40506-0055, USA, and [b]Department of Chemistry and Biochemistry, Ohio State University, Columbus, OH 43210, USA
Correspondence e-mail: s.parkin@uky.edu

Received 6 June 2011
Accepted 1 July 2011
Online 27 July 2011

Crystals of 5-hydroxy-6-methyl-2-pyridone, (I), grown from a variety of solvents, are invariably trigonal (space group $R\overline{3}$); these are 5-hydroxy-6-methyl-2-pyridone acetone 0.1667-solvate, $C_6H_7NO_2\cdot0.1667C_3H_6O$, (I*a*), and 6-methyl-5-hydroxy-2-pyridone propan-2-ol 0.1667-solvate, $C_6H_7NO_2\cdot0.1667C_3H_8O$, (I*b*), and the forms from methanol, (I*c*), water, (I*d*), benzonitrile, (I*e*), and benzyl alcohol, (I*f*). They incorporate channels running the length of the *c* axis that contain extensively disordered solvent molecules. A solvent-free sublimed powder of 5-hydroxy-6-methyl-2-pyridone microcrystals is essentially isostructural. Inversion-related host molecules interact *via* pairs of N—H···O hydrogen bonds to form $R_2^2(8)$ dimers. Six of these dimers form large $R_{12}^6(42)$ puckered rings, in which the O atom of each N—H···O hydrogen bond is also the acceptor in an O—H···O hydrogen bond that involves the 5-hydroxy group. The large $R_{12}^6(42)$ rings straddle the $\overline{3}$ axes and form stacked columns *via* π–π interactions between inversion-related molecules of (I) [mean interplanar spacing = 3.254 Å and ring centroid–centroid distance = 3.688 (2) Å]. The channels are lined by methyl groups, which all point inwards to the centre of the channels.

Comment

^{1}H NMR data obtained from crystals of 5-hydroxy-6-methyl-2-pyridone, (I) (Behrman, 2008, 2009), grown from acetone or propan-2-ol, exhibit unusual, and sometimes variable, ratios of pyridone to solvent. A similar observation for the 6-chloro analogue was established as being due to the presence of continuous solvent-accessible channels formed by extensive hydrogen-bonding networks within the crystals (Parkin & Behrman, 2009). The tautomeric equilibrium in the 6-chloro analogue was sensitive to the molecular environment, such that solvate crystals were exclusively the hydroxy tautomer while solvent-free crystals were the pyridone. Studies of related 6-substituted 2-pyridones over many years (summarized by Nichol & Clegg, 2005) show that electron-donating substituents at the 6-position drive the tautomeric equilibrium towards the pyridone, while electron-withdrawing groups favour the hydroxy form. In the present work, we found no evidence of the corresponding 6-methyl-2,5-dihydroxypyridine, (II).

Current work on intrinsic and extrinsic porous organic molecules has been the subject of several recent reviews, most notably by Cooper and coworkers (Holst *et al.*, 2010; Cooper, 2011; Mastalerz *et al.*, 2011; Jones *et al.*, 2011). Given the general interest in hydrogen-bonded assemblies (*e.g.* Sisson *et al.*, 2005; Glidewell *et al.*, 2005; Hao *et al.*, 2005) and keto/enol tautomerism in 6-pyridones (Almlöf *et al.*, 1971; Kvick, 1976; Johnson, 1984), we undertook a study of (I) crystallized from a series of solvents. We report here the structures of crystals grown from acetone, (I*a*), propan-2-ol, (I*b*), methanol, (I*c*), water, (I*d*), and benzonitrile, (I*e*). A probable structure grown from benzyl alcohol, (I*f*), and a solvent-free crystalline powder obtained by sublimation, (I*g*), are also discussed. Crystallographic data are only presented here for structures (I*a*) and (I*b*); data for structures (I*c*1), (I*c*2), (I*c*3), (I*d*) and (I*e*) are available in the *Supplementary materials*.

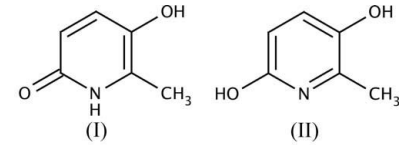

(I*a*) = (I)·0.167C_3H_6O
(I*b*) = (I)·0.167C_3H_8O

In contrast with the 6-chloro analogue, which formed tetragonal crystals (space group $I4_1/a$) with four channels per unit cell, all crystals of (I) are trigonal, space group $R\overline{3}$, and have three channels per unit cell. The host-molecule frameworks in (I*a*)–(I*e*), and likely also in (I*f*) and (I*g*), are isostructural. Given the similarities, the following section concentrates on the structure of (I*a*). Unless otherwise noted, the general features (aside from the nature of the solvent) also apply to (I*b*)–(I*e*), and probably also to (I*f*) and (I*g*).

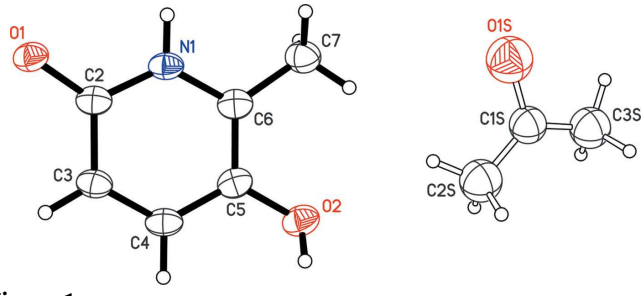

Figure 1
The asymmetric unit of the acetone solvate, (I*a*), showing the atom-numbering scheme. Displacement ellipsoids are drawn at the 50% probability level. The acetone guest molecule, which was modelled with isotropic displacement parameters, sits on a site of $\overline{3}$ symmetry and is extensively disordered. The structures of the propan-2-ol, methanol, water and benzonitrile solvates, (I*b*)–(I*e*), are essentially the same, but the guest solvent molecule in each of (I*c*)–(I*e*) was too badly disordered to model.

  doi:10.1107/S0108270111026254

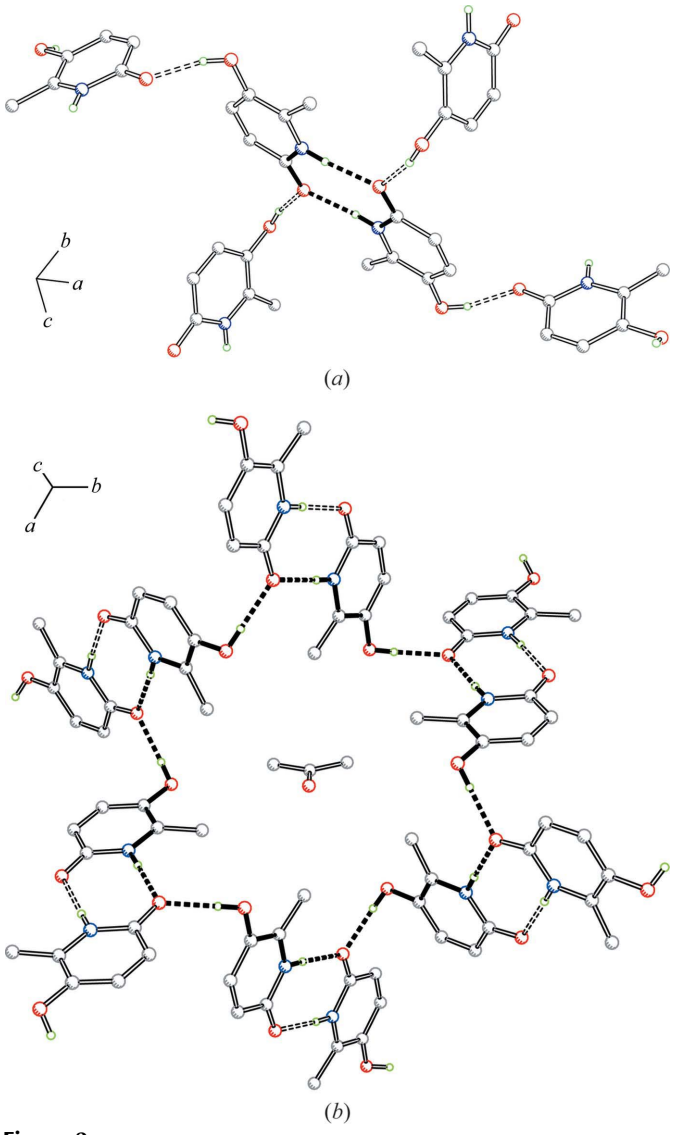

Figure 2
The hydrogen bonding in (I*a*), showing (*a*) the molecules forming $R_2^2(8)$ inversion-related dimers *via* pairs of N—H···O hydrogen bonds, and (*b*) six sets of these hydrogen-bonded dimers forming puckered rings, in which the O atom of each N—H···O interaction is also the acceptor in an O—H···O hydrogen bond involving the 5-hydroxy group as donor. The 6-Me groups all point towards the centres of the large rings. The resulting large $R_{12}^6(42)$ rings straddle the $\overline{3}$ axis and stack to form solvent-accessible channels parallel to the *c* axis.

The molecular structure of (I*a*) (Fig. 1) is largely unremarkable. Bond lengths and angles are all within normal ranges and the molecules are flat [the r.m.s. deviation from planarity is 0.0140 (16) Å for non-H atoms]. The 2-hydroxy H atom is oriented away from the 6-methyl group, but is twisted out of the plane of the ring by *ca* 43° so as to participate in an O2—H2···O1($-y+\frac{4}{3}$, $x-y+\frac{2}{3}$, $z+\frac{2}{3}$) hydrogen bond to a symmetry-related molecule (Table 2). Inversion-related molecules of (I) interact *via* pairs of N1—H1···O1 hydrogen bonds to form $R_2^2(8)$ dimers (Fig. 2*a*) (for graph-set notation, see Bernstein *et al.*, 1995). Six of these dimers join to form puckered rings (Fig. 2*b*) in which atom O1 of each N1—H1···O1 hydrogen bond is also the acceptor in an O2—H2···O1 hydrogen bond. The resulting large $R_{12}^6(42)$ rings surround the $\overline{3}$ axes and stack into columns *via* π–π interactions between inversion-related molecules of (I) [mean π–π spacing = 3.254 (2) Å and ring centroid–centroid distance = 3.688 (2) Å]. The channels are lined with 6-methyl groups which point towards the centre of their respective $R_{12}^6(42)$ rings. Appropriately sized solvent molecules can occupy the channels, but on average they are severely disordered as a result of the $\overline{3}$ site symmetry within the channels (Fig. 3). In spite of the inherent disorder, it was possible to model the acetone and propan-2-ol molecules in (I*a*) and (I*b*), albeit with extensive use of restraints (see *Refinement*). These models had (in total) one solvent molecule per channel per unit cell. The occupancies of the solvent models were allowed to refine, but in both (I*a*) and (I*b*), the summed site occupancy of all disorder components was so close to unity that the solvent in the final cycles of refinement was fixed at full occupancy.

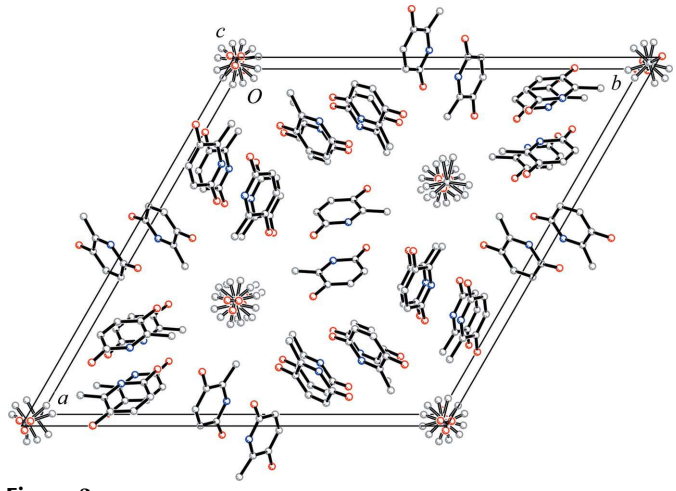

Figure 3
A packing diagram for (I*a*), viewed along *c*, showing the presence of disordered guest solvent molecules within the channels parallel to *c*. Crystals of (I*b*)–(I*e*) exhibit essentially the same packing.

Although reasonably sized crystals could be grown from a variety of solvents, satisfactory disorder models for smaller solvents such as methanol in (I*c*) and water in (I*d*) were not readily constructed. Crystals from methanol or water do appear to hold solvent less tightly, so that the solvent content varies depending on the method of drying (*i.e.* in air, *in vacuo* or at 373 K) from *ca* 2.5 molecules per channel per unit cell to less than one. A room-temperature determination of the methanol-containing structure, (I*c*2), revealed no substantive differences from the low-temperature model, (I*c*1). An attempt to drive the methanol guest molecules from the channels in (I*c*) by annealing at 381 K for *ca* 30 min was also performed. In the resulting structure, (I*c*3), the channels remained intact, though they appear to be partially depopulated. The electron count within the channels, as calculated by the SQUEEZE routine in *PLATON* (Spek, 2009), was reduced from 46 e in (I*c*1) to 24 e in (I*c*3), but it is worth mentioning that the electron count for the room-temperature structure, (I*c*2), was only 10 e. This variability is consistent with peak integrations of the ^{1}H NMR spectra for different

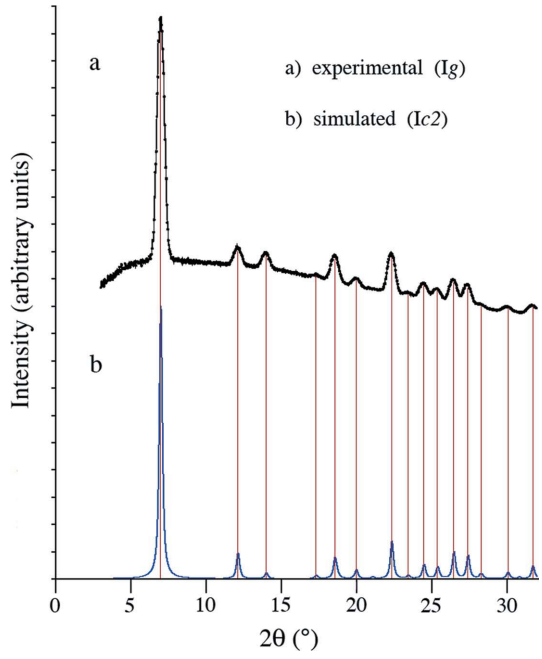

Figure 4
Qualitative comparison of powder diffraction patterns of (I). (*a*) Experimental pattern from sublimed powder, (I*g*), at room temperature. Radial integration from two-dimensional diffraction images (see *Supplementary materials*). (*b*) Simulated pattern, based on the room-temperature single-crystal structure, (I*c*2). The thin vertical lines are intended merely to guide the eye.

samples of (I*c*). We surmise that some small solvent species are able to vacate the channels to a degree that depends on crystal handling, treatment and environment. Crystallization from benzonitrile produced a similar structure, (I*e*), but with shorter and broader channels (as evidenced by the cell dimensions), presumably to accommodate this larger molecule. Crystals grown from benzyl alcohol, (I*f*), were too small for full data collection, but indexing of a miniscule crystal of (I*f*) (*ca* 0.1 × 0.005 × 0.005 mm) revealed a trigonal unit cell similar to the other crystals.

All attempts to grow solvent-free crystals large enough for single-crystal work by sublimation up to *ca* 423 K were unsuccessful and resulted in a fine white powder, (I*g*). Diffraction of Cu $K\alpha$ X-rays by this sublimed powder was too weak to measure on conventional sealed-tube powder X-ray diffractometers. However, it was possible to collect two-dimensional diffraction images on a rotating-anode-based Bruker X8 Proteum single-crystal diffractometer equipped with graded multilayer optics. Diffraction patterns from freshly sublimed (I*g*) and from (I*g*) that had aged undisturbed for about six months were essentially identical (see *Supplementary materials*). These two-dimensional images were radially integrated using *DATASQUEEZE* (Heiney, 2005) and compared with simulated powder patterns based on the single-crystal structures (calculated using *Mercury*; Macrae *et al.*, 2008), as shown in Fig. 4. Diffraction peak positions from the sublimed powders are in excellent agreement with those in the simulated powder patterns. It is consistent with this that the IR spectrum of the sublimed material is identical to spectra of the solvent-containing crystals, within the limits of detection. It thus appears that the channel structure is maintained even in the absence of intrinsic solvent, in marked contrast with the 6-chloro crystals, which were found to collapse on solvent loss (Parkin & Behrman, 2009). Holst *et al.* (2010) regard molecular crystals that retain permanent micropore structures upon desolvation as atypical. We also considered that the channels of the sublimed material might have contained air. Elemental analysis showed no increase in the percentage of nitrogen; even one molecule of N_2 per unit cell would have been easily detectable. Thus, the channels in the sublimed powder are essentially empty. ^{1}H NMR spectra showed solvent–host ratios consistent with the X-ray data. A few other 6-substituted 5-hydroxy-2-pyridones were examined but these did not form channels: 6-H (Behrman, 2008), 6-Br [Eikhoff & Behrman, 2009 (see *Supplementary materials*); Smith, 1951; Newkome *et al.*, 1974] and 6-nitroso (Krowicki, 1977).

Experimental

The synthesis of 5-hydroxy-6-methyl-2-pyridone has been described in several publications (Behrman, 2008; Loth & Hempel, 1972). Crystals of (I*a*) suitable for X-ray diffraction analysis were prepared by dissolving (I) (100 mg) in hot ethanol (6 ml) and then slowly adding acetone (10 ml). The other solvates were prepared as follows (mass of 5-hydroxy-6-methyl-2-pyridone, volume of solvent): (I*b*) 50 mg, 5 ml propan-2-ol; (I*c*) 50 mg, 3 ml methanol; (I*d*) 50 mg, 2 ml water; (I*e*) 50 mg, 3.5 ml benzonitrile; (I*f*) 20 mg, 0.5 ml benzyl alcohol. Crystals from benzonitrile and benzyl alcohol were washed with diethyl ether. Sublimation was carried out at about 0.5 mm Hg and at a temperature gradually rising from room temperature to about 423 K. ^{1}H NMR spectra were measured in DMSO-d_6 at 600 MHz. They gave host–solvent ratios consistent with disordered model refinement for the acetone and propan-2-ol solvates, or from a count of the number of electrons present within the channels using SQUEEZE in *PLATON* (Spek, 2009). Data for the IR, UV and NMR spectra are given by Behrman (2008) and Loth & Hempel (1972).

Compound (I*a*), acetone solvate

Crystal data

$C_6H_7NO_2{\cdot}0.1667C_3H_6O$
M_r = 134.81
Trigonal, $R\overline{3}$
a = 24.7962 (3) Å
c = 5.2924 (1) Å
V = 2818.08 (7) Å^3
Z = 18
Cu $K\alpha$ radiation
μ = 0.91 mm^{-1}
T = 90 K
0.12 × 0.01 × 0.01 mm

Data collection

Bruker X8 Proteum diffractometer
14372 measured reflections
1153 independent reflections
854 reflections with $I > 2\sigma(I)$
R_{int} = 0.077

Refinement

$R[F^2 > 2\sigma(F^2)]$ = 0.044
$wR(F^2)$ = 0.130
S = 1.03
1153 reflections
101 parameters
6 restraints
H-atom parameters constrained
$\Delta\rho_{max}$ = 0.17 e Å^{-3}
$\Delta\rho_{min}$ = −0.39 e Å^{-3}

Table 1
Selected geometric parameters (Å, °) for (I*a*).

N1—C2	1.365 (3)	C4—C5	1.401 (3)
N1—C6	1.368 (3)	C5—O2	1.368 (3)
C2—O1	1.276 (3)	C5—C6	1.373 (3)
C2—C3	1.416 (3)	C6—C7	1.485 (3)
C3—C4	1.366 (3)		
C2—N1—C6	125.66 (18)	O2—C5—C6	119.4 (2)
O1—C2—N1	119.29 (18)	O2—C5—C4	121.95 (19)
O1—C2—C3	125.0 (2)	C6—C5—C4	118.6 (2)
N1—C2—C3	115.68 (19)	N1—C6—C5	118.2 (2)
C4—C3—C2	120.0 (2)	N1—C6—C7	117.13 (19)
C3—C4—C5	121.9 (2)	C5—C6—C7	124.7 (2)

Table 2
Hydrogen-bond geometry (Å, °) for (I*a*).

D—H···*A*	*D*—H	H···*A*	*D*···*A*	*D*—H···*A*
N1—H1···O1^{i}	0.88	1.90	2.781 (2)	174
O2—H2···O1^{ii}	0.84	1.81	2.634 (2)	165

Symmetry codes: (i) $-x+1, -y+1, -z$; (ii) $-y+\frac{4}{3}, x-y+\frac{2}{3}, z+\frac{2}{3}$.

Table 3
Selected geometric parameters (Å, °) for (I*b*).

N1—C2	1.365 (3)	C4—C5	1.403 (3)
N1—C6	1.369 (3)	C5—O2	1.364 (3)
C2—O1	1.277 (3)	C5—C6	1.375 (3)
C2—C3	1.417 (3)	C6—C7	1.486 (3)
C3—C4	1.366 (3)		
C2—N1—C6	125.54 (18)	O2—C5—C6	119.6 (2)
O1—C2—N1	119.25 (18)	O2—C5—C4	121.73 (19)
O1—C2—C3	125.11 (19)	C6—C5—C4	118.6 (2)
N1—C2—C3	115.65 (18)	N1—C6—C5	118.31 (19)
C4—C3—C2	120.2 (2)	N1—C6—C7	117.04 (19)
C3—C4—C5	121.7 (2)	C5—C6—C7	124.6 (2)

Table 4
Hydrogen-bond geometry (Å, °) for (I*b*).

D—H···*A*	*D*—H	H···*A*	*D*···*A*	*D*—H···*A*
N1—H1···O1^{i}	0.88	1.91	2.782 (2)	174
O2—H2···O1^{ii}	0.84	1.81	2.638 (2)	169

Symmetry codes: (i) $-x+1, -y+1, -z$; (ii) $-y+\frac{4}{3}, x-y+\frac{2}{3}, z+\frac{2}{3}$.

Compound (I*b*), propan-2-ol solvate

Crystal data

$C_6H_7NO_2\cdot 0.1667C_3H_8O$
M_r = 135.14
Trigonal, $R\overline{3}$
a = 24.9208 (5) Å
c = 5.2738 (1) Å
V = 2836.47 (10) Å^3
Z = 18
Cu $K\alpha$ radiation
μ = 0.90 mm^{-1}
T = 90 K
0.13 × 0.01 × 0.01 mm

Data collection

Bruker X8 Proteum diffractometer
14474 measured reflections
1163 independent reflections
908 reflections with $I > 2\sigma(I)$
R_{int} = 0.071

Refinement

$R[F^2 > 2\sigma(F^2)]$ = 0.047
$wR(F^2)$ = 0.132
S = 1.07
1163 reflections
101 parameters
11 restraints
H-atom parameters constrained
$\Delta\rho_{max}$ = 0.27 e Å^{-3}
$\Delta\rho_{min}$ = −0.30 e Å^{-3}

H atoms of the molecules of (I) in each of the structures were found in difference Fourier maps and subsequently placed at idealized positions. For the low-temperature structures, riding models with constrained distances of 0.95 ($C_{Ar}H$), 0.98 (RCH_3), 0.88 (NH) and 0.84 Å (OH) were used. For the room-temperature structure, (I*c*2), the distances were 0.93 ($C_{Ar}H$), 0.96 (RCH_3), 0.86 (NH) and 0.82 Å (OH). In (I*a*) and (I*b*), owing to extensive disorder, the H atoms of the solvent molecules were not found in difference maps. They were placed using geometric criteria and refined using riding models, with constrained distances of 0.98 (RCH_3), 0.99 (R_2CH_2) and 0.84 Å (OH). Values for U_{iso}(H) were set at 1.2U_{eq}(parent atom), or at 1.5U_{eq}(parent atom) for OH and CH_3. We considered including the structures processed using SQUEEZE (*PLATON*; Spek, 2009), but there seemed little point as they would have added no additional insight.

In (I*a*) and (I*b*), the solvent molecules are disordered on sites of $\overline{3}$ point symmetry and required restraints to maintain chemically sensible geometry and physically reasonable displacement parameters. The *SHELXL97* (Sheldrick, 2008) commands DFIX, SAME, FLAT and SIMU were used to restrain interatomic distances, maintain geometric similarity and flatness, and keep the displacement parameters of closely proximate atoms similar. In both (I*a*) and (I*b*), several different disorder models were tried. The best model in each case was chosen by visual inspection and by careful analysis of refinement statistics, including an R tensor (Parkin, 2000), which quantifies the spatial quality of a crystallographic refinement. In (I*c*1), (I*c*2), (I*c*3), (I*d*) and (I*e*), the solvent molecules were also disordered on sites of $\overline{3}$ point symmetry, but suitable disorder models were not constructed.

Data collection: *APEX2* (Bruker, 2006) for (I*a*), (I*b*), (I*d*) and (I*e*); *COLLECT* (Nonius, 1998) for (I*c*1), (I*c*2) and (I*c*3). Cell refinement: *APEX2* for (I*a*), (I*b*), (I*d*) and (I*e*); *SCALEPACK* (Otwinowski & Minor, 1997) for (I*c*1), (I*c*2) and (I*c*3). Data reduction: *APEX2* for (I*a*), (I*b*), (I*d*) and (I*e*); *DENZO-SMN* (Otwinowski & Minor, 1997) for (I*c*1), (I*c*2) and (I*c*3). For all compounds, program(s) used to solve structure: *SHELXS97* (Sheldrick, 2008); program(s) used to refine structure: *SHELXL97* (Sheldrick, 2008); molecular graphics: *XP* in *SHELXTL* (Sheldrick, 2008); software used to prepare material for publication: *SHELXL97* and local procedures.

The authors are grateful to the late Dr Charles Cottrell for his NMR expertise, and to Dr Henry Francis for advice on powder X-ray diffraction. X-ray data were collected at the University of Kentucky, using both a Nonius KappaCCD diffractometer purchased with University funds and a Bruker Nonius X8 Proteum diffractometer obtained with funding from the NSF (MRI grant No. 0319176).

Supplementary materials for this paper are available from the IUCr electronic archives (Reference: MX3051). Services for accessing these data are described at the back of the journal.

References

Almlöf, J., Kvick, Å. & Olovsson, I. (1971). *Acta Cryst.* B**27**, 1201–1208.
Behrman, E. J. (2008). *Synth. Commun.* **38**, 1168–1175.

Behrman, E. J. (2009). *Synth. Commun.* **39**, 3378.
Bernstein, J., Davis, R. E., Shimoni, L. & Chang, N.-L. (1995). *Angew. Chem. Int. Ed. Engl.* **34**, 1555–1573.
Bruker (2006). *APEX2*. Bruker AXS Inc., Madison, Wisconsin, USA.
Cooper, A. I. (2011). *Angew. Chem. Int. Ed.* **50**, 996–998.
Eikhoff, N. & Behrman, E. J. (2009). Unpublished; see *Supplementary materials*.
Glidewell, C., Low, J. N., Skakle, J. M. S. & Wardell, J. L. (2005). *Acta Cryst.* C**61**, o493–o495.
Hao, X., Parkin, S. & Brock, C. P. (2005). *Acta Cryst.* B**61**, 689–699.
Heiney, P. (2005). *Commission on Powder Diffraction Newsletter*, **32**, 9–11.
Holst, J. R., Trewin, A. & Cooper, A. I. (2010). *Nat. Chem.* **2**, 915–920.
Johnson, C. D. (1984). *Comprehensive Heterocyclic Chemistry*, Vol. 2, edited by A. R. Katritzky & C. W. Rees, pp. 148–157. Oxford: Pergamon.
Jones, J. T. A., Holden, D., Mitra, T., Hasell, T., Adams, D. J., Jelfs, K. E., Trewin, A., Willock, D. J., Day, G. M., Bacsa, J., Steiner, A. & Cooper, A. I. (2011). *Angew. Chem. Int. Ed.* **50**, 749–753.
Krowicki, K. (1977). *Rocz. Chem.* **51**, 1035–1040.
Kvick, Å. (1976). *Acta Cryst.* B**32**, 220–224.
Loth, H. & Hempel, B. (1972). *Arch. Pharm.* **305**, 724–731.
Macrae, C. F., Bruno, I. J., Chisholm, J. A., Edgington, P. R., McCabe, P., Pidcock, E., Rodriguez-Monge, L., Taylor, R., van de Streek, J. & Wood, P. A. (2008). *J. Appl. Cryst.* **41**, 466–470.
Mastalerz, M., Schneider, M. W., Oppel, I. M. & Presly, O. (2011). *Angew. Chem. Int. Ed.* **50**, 1046–1051.
Newkome, G. R., Broussard, J., Staires, S. K. & Sauer, J. D. (1974). *Synthesis*, p. 707.
Nichol, G. S. & Clegg, W. (2005). *Acta Cryst.* C**61**, o383–o385.
Nonius (1998). *COLLECT*. Nonius, BV, Delft, The Netherlands.
Otwinowski, Z. & Minor, W. (1997). *Methods in Enzymology*, Vol. 276, *Macromolecular Crystallography*, Part A, edited by C. W. Carter Jr & R. M. Sweet, pp. 307–326. New York: Academic Press.
Parkin, S. (2000). *Acta Cryst.* A**56**, 157–162.
Parkin, S. R. & Behrman, E. J. (2009). *Acta Cryst.* C**65**, o529–o533.
Sheldrick, G. M. (2008). *Acta Cryst.* A**64**, 112–122.
Sisson, A. L., Sanchez, V. D. A., Magro, G., Griffin, A. M. E., Shah, S., Charmant, J. P. H. & Davis, A. P. (2005). *Angew. Chem. Int. Ed.* **44**, 6878–6881.
Smith, J. N. (1951). *J. Chem. Soc.* pp. 2861–2863.
Spek, A. L. (2009). *Acta Cryst.* D**65**, 148–155.